Physica B 156 & 157 (1989) 437–443
North-Holland, Amsterdam

CHAPTER 11 MACROMOLECULES AND BIOLOGICAL SYSTEMS

INTERNAL DYNAMICS OF GLOBULAR PROTEINS: COMPARISON OF NEUTRON SCATTERING MEASUREMENTS AND THEORETICAL MODELS

Jeremy SMITH[1], Krzysztof KUCZERA[1,*], Bruce TIDOR[1], Wolfgang DOSTER[2], Stephen CUSACK[3] and Martin KARPLUS[1]

[1]*Chemistry Department, Harvard University, 12 Oxford St., Cambridge, MA 02138, USA*
[2]*Technische Universität München, Physik-Department E13, D-8046 Garching, Fed. Rep. Germany*
[3]*E.M.B.L., c/o/ ILL, Avenue des Martyrs, 156X, 38042 Grenoble Cedex, France*

Invited paper

The picosecond internal dynamics of globular proteins are explored by measuring inelastic neutron scattering and comparing the results with theoretical models. For frequencies below 200 cm^{-1}, the spectra from different proteins are similar under the same experimental conditions. At low temperatures or hydration the dynamics are approximately harmonic, whereas at high temperatures or hydration there is considerable quasielastic scattering. The quasielastic scattering can be explained by a shift of the density of states to lower frequencies with increased friction, but picosecond timescale transitions between slightly different conformations might also contribute. Spectra calculated from molecular dynamics simulations of myoglobin at 80 K and 300 K approximately reproduce the observed changes with temperature. The simulations show evidence for restriction of the conformational space sampled at 80 K, relative to 300 K.

1. Introduction

Globular proteins exhibit a wide variety of internal motions, ranging from high frequency bond stretching vibrations to longer timescale diffusive and activated phenomena [1, 2]. Some of these motions are important for the biological function [1].

Picosecond timescale (3–200 cm^{-1}) dynamics are of particular interest because they dominate the mean squared displacements of atoms from their equilibrium positions. They tend to be global in nature, involving correlated motions of groups of atoms. Research on picosecond protein dynamics has mostly been theoretical, employing empirical energy functions to compute normal modes or perform molecular dynamics simulations [1, 2]. Few experimental data exist on such fundamental characteristics as the frequencies of the motions involved and the degree of damping and anharmonicity. Inelastic neutron scattering, the incoherent part of which is determined by self-correlations in hydrogen motions in proteins, is well suited to address such problems.

In this paper we present the results of inelastic neutron scattering experiments which, aided by comparisons with theoretical models, allow some general conclusions to be reached concerning the nature of picosecond protein motions as a function of the environment. In section 2, experimental spectra and theoretical models are presented to investigate the picosecond dynamics of proteins as a function of temperature and hydration. It is found that harmonic dynamics can largely explain the data at low temperatures and hydrations, whereas there is additional strong quasielastic scattering at high temperatures/hydrations. The origins of this quasielastic component are discussed. The conclusions are stated in section 3.

2. Methods and results

2.1. Experimental spectra from BPTI and lysozyme powders

Inelastic spectra were measured from BPTI and lysozyme which had been twice lyophilised from D_2O, to final hydrations of 0.12 and

* On leave from: Institute of Physics, Polish Academy of Sciences, Al.Lotnikow 32/46, 02-668 Warsaw, Poland.

0921-4526/89/$03.50

0.04 g D_2O/g protein, respectively. Spectra were measured on the spectrometer IN6 at the ILL. Fuller details will be published elsewhere [3]. Corrected time of flight spectra for the BPTI and lysozyme samples are presented in figs. 1(a) and 1(b). These spectra have the typical form characteristic of globular proteins [4–6]. They are similar in the low frequency region (0–200 cm^{-1}) but show differences at higher frequencies. The neutron derived density of states, $G(\omega)$, was obtained from the data by extrapolation to $q = 0$ for the BPTI powder using a method which accounts for multiple scattering [7]. It is shown as the line of circles in fig. 2; the density of states rises relatively smoothly to a maximum at about 125 cm^{-1}.

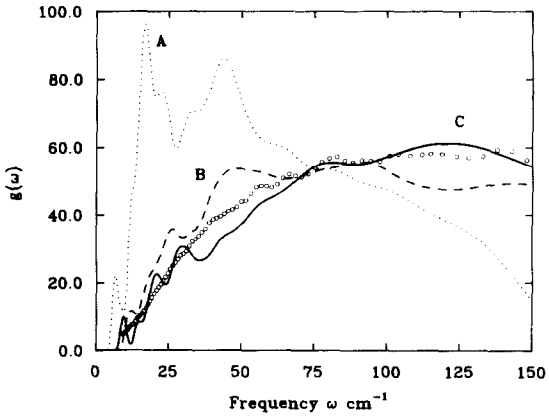

Fig. 2. Densities of states from the BPTI powder experiment, fig. 1(a), and from three normal mode analyses computed with program CHARMM. The experimental curve is given by the circles. Model A (dotted line) uses shift electrostatics and the extended atom approximation, model B (dashed line) uses switch electrostatics and the extended atom approximation, and model C (solid line) uses switch electrostatics and explicitly includes all of the atoms.

2.2. *g(ω) from different harmonic models of BPTI*

Calculations have shown that, at present instrumental resolutions, the neutron derived $G(\omega)$, although weighted by the hydrogen normal mode displacement vectors, is similar in form to the unweighted density of states, $g(\omega)$, [8], the fundamental physical quantity from which dynamic effects on the thermodynamics of biological processes can be determined.

It is of interest to compare the frequency distributions calculated from different dynamical models with the experimentally obtained $G(\omega)$. To this end, three normal mode analyses of BPTI were performed with the molecular mechanics program CHARMM [9]. This involved energy minimising the BPTI crystal structure [10] and evaluating the force constant matrix. The normal mode analyses were performed in Cartesian coordinates with this matrix.

The analyses differ from each other in two respects. The first difference concerns truncation of the long range electrostatic interactions, which

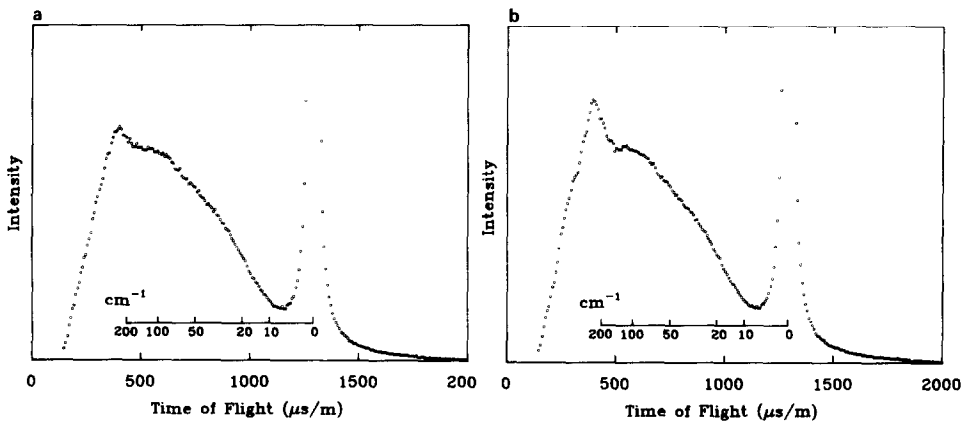

Fig. 1. Time of flight spectra from lyophilised BPTI (a) and lysozyme (b) powders at 66.6° scattering angle. The incident wavelength was 5.14 Å. The data was treated using the program CROSSX at the ILL [24] including subtraction of the cell scattering and the application of slab transmission corrections.

is necessary to make the calculations computationally feasible. Two truncation methods are commonly employed for calculations on proteins, the 'shift' and 'switch' [9] methods. In the shift method, electrostatic interactions are reduced to zero at the cutoff distance (here 7.5 Å) by shifting the potential in such a way that the first derivative is also equal to zero. For the 'switch' method the truncation is performed by multiplying each term by a cubic switching function; here, this function is unity for a distance less than 6.5 Å, zero for a distance greater than 7.5 Å, and interpolates smoothly between the two.

The second difference involves the treatment of the nonpolar hydrogens. In the 'extended atom' approximation [9], only polar hydrogens are explicitly included and the aliphatic hydrogens are treated as part of the carbon atoms to which they are attached. Such extended atoms have modified nonbonded parameters and the appropriate masses. This procedure reduces the number of atoms in the system from 904 to 580, decreasing the computational requirements.

Densities of states computed from the normal mode analyses are shown in fig. 2. Model A (dotted line), a description of which has been published previously [11], uses the shift method of electrostatic truncation with the extended atom approximation. Model B (dashed line) uses the switch method with the extended atom approximation, and model C (solid line) uses the switch method but explicitly includes all of the atoms. To enable direct comparison with the experimental curve, the calculated $g(\omega)$'s have been convoluted with the instrumental resolution function of IN6.

Fig. 2 demonstrates that the method of electrostatic truncation used has an important effect on the distribution of low frequency modes. Overall, use of the shift function lowers the frequencies of the very low frequency modes ($<75\ \mathrm{cm}^{-1}$), relative to those calculated with the switch function. Comparison with the experimentally derived $G(\omega)$ shows that the normal modes calculated including all the atoms explicitly and with switch electrostatics are in best agreement with experiment.

2.3. *Time of flight spectra for BPTI powder – inclusion of frictional damping*

The mode frequencies and amplitude vectors from the preferred normal mode model (model C) were used for calculation of time of flight spectrum. The time of flight spectrum presented in fig. 3 (dotted line) was obtained by convolution of the calculated $S(q, \omega)$ with the instrumental resolution function of IN6, and is directly comparable to fig. 1(a). A detailed description of the scattering expected from harmonic protein dynamics has been published [8, 12, 13]. The general features of the experimental spectrum are reproduced by model C. However, the experimental spectrum is slightly convex in the region 20–75 cm^{-1} whereas the calculated spectrum is concave. This is due to a greater density of states in this region in the experimental sample (see fig. 2). The other major difference is that the experimental spectrum is smoother than that calculated from the harmonic model.

It is possible that internal frictional effects might contribute to the smoother observed scattering. The effect of damping of the normal modes can be approximated by treating each mode as an independent damped Langevin oscillator [13, 14]. We find that to produce improved agreement with fig. 1, the low frequency modes

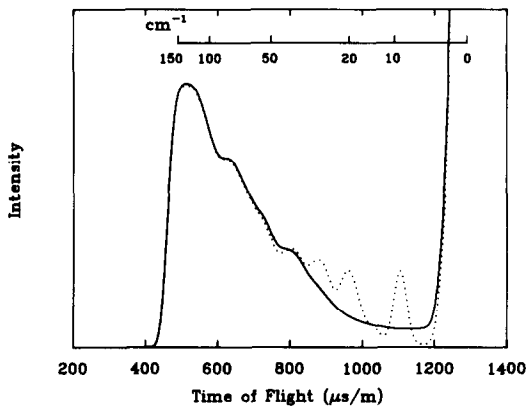

Fig. 3. Time of flight spectra calculated from harmonic model C, with (solid line) and without (dotted line) frictional damping. The frictional damping is included by assuming each mode to be an independent damped Langevin oscillator with a friction constant $f(\omega)$ in cm^{-1} given by $f(\omega) = 30.0 \exp[-\omega^2/450]$.

must be overdamped. A spectrum calculated with such a frictional coefficient distribution is presented in fig. 3 (solid line). The increased smoothness of the calculated spectrum is in closer accord with the experimental spectrum of fig. 1(a).

2.4. Dynamical effects of solvation of BPTI

$S(q, \omega)$ from the BPTI powder experiment described in section 2.1. is shown in fig. 4(a), and from exchanged BPTI in D_2O solution in fig. 4(b). The broadening effect due to translational diffusion of the molecules is small [5]. The peak in the powder $S(q, \omega)$ is not present in the solvated molecule scattering, which is primarily quasielastic.

For a protein molecule in solution, there are at least two separate solvent effects on the protein dynamics. The equilibrium positions of the atoms in the protein can be altered resulting in a change in the density of states and accompanying atomic amplitudes. In addition, increased frictional damping can occur from solvent–protein atom collisions. $S(q, \omega)$ calculated using the damped oscillator model of fig. 3 is presented in fig. 5(a). As in the experimental results, there is a peak in $S(q, \omega)$, although this is at a higher frequency in the calculated spectrum, reflecting the relative lack of modes between 20 and 40 cm^{-1} mentioned in the previous section, with perhaps too strong damping in this region. We have investigated how this model, which approximately reproduces the low hydration powder data, must be modified to reproduce the change in $S(q, \omega)$ on solvation of BPTI. We found that the density of states must be shifted to low frequencies. Indeed, by assuming the distribution of frequencies obtained using the harmonic model A of section 2.2, which has more modes at low frequencies, and by increasing the frictional damping, the solvent effect on $S(q, \omega)$ can be approximately reproduced (fig. 5(b)).

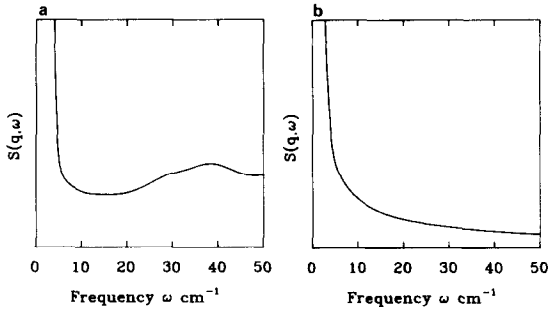

Fig. 5. Simulation of solvent effect using a damped harmonic model. $S(q, \omega)$ for the damped harmonic model C is shown in fig. 5(a). Fig. 5(b) uses the density of states from model A of fig. 2 with a friction constant of 30 cm^{-1} for each mode.

2.5. Temperature dependence of myoglobin dynamics

Experimental $S(q, \omega)$ plots for myoglobin at 100 K and 300 K are presented in figs. 6(a) and 6(b). On increasing temperature a similar effect is seen to that observed on increasing hydration; i.e. the scattering is predominantly due to vibra-

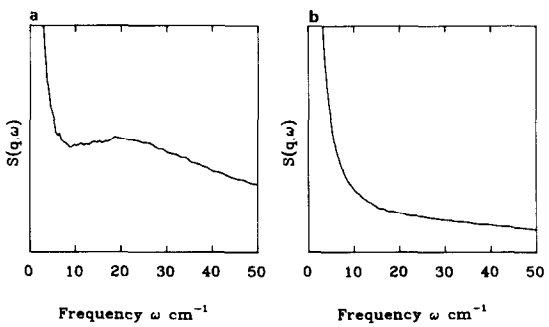

Fig. 4. $S(q, \omega)$ for BPTI in powder (a) and D_2O solution (b) forms. The scattering from the molecule in solution was obtained using the same procedure as figs. 1(a) and 1(b), with the solvent contribution subtracted. The concentration was 164 mg/ml.

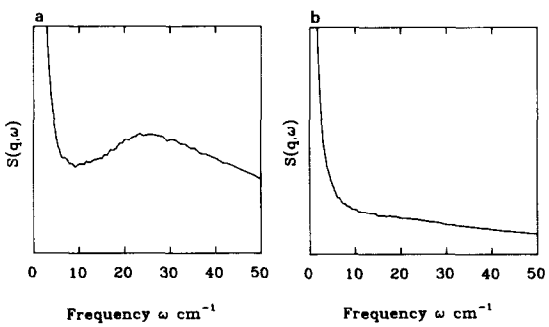

Fig. 6. Experimental $S(q, \omega)$ at constant angle (180°) for myoglobin powder (0.33 g/g hydration) at 100 K (a) and 300 K (b). The spectra were measured on IN6 with an incident wavelength of 5.14 Å.

tional modes (as evidenced by the peak in $S(q, \omega)$ and the relative absence of quasielastic scattering) at low temperatures, but is more quasielastic at high temperatures. A full analysis of the temperature dependence of the experimental myoglobin scattering will be presented elsewhere [15].

It has been proposed that protein molecules might exist in many conformational 'substates' [16–18], which are slightly different conformations that can be adopted by the protein at 300 K while maintaining the same overall structure. Transitions between substates would involve potential energy barrier crossing, resulting in proteins being more restricted in conformational space at low temperatures.

Protein conformational substates can be explored using molecular dynamics simulations [18]. These simulations provide a more complete picture of protein dynamics than harmonic or damped harmonic models, which neglect anharmonic and activated motions.

In figs. 7(a) and 7(b) $S(q, \omega)$ are presented calculated from molecular dynamics simulations of myoglobin at 80 K and at 300 K (120 ps and 50 ps duration respectively). The 80 K trajectory was obtained by quenching the 300 K trajectory. The form of the scattering at 300 K (fig. 7(b)) is indicative of quasielastic processes dominating the picosecond timescale fluctuations. At 80 K the calculated scattering indicates that the dynamics is predominantly harmonic, in agreement with the experimental results. Fig. 7(a) shows a clear peak in the spectrum just below 20 cm^{-1}. The peak is sharper and shifted to somewhat lower frequencies compared to the experimental peak.

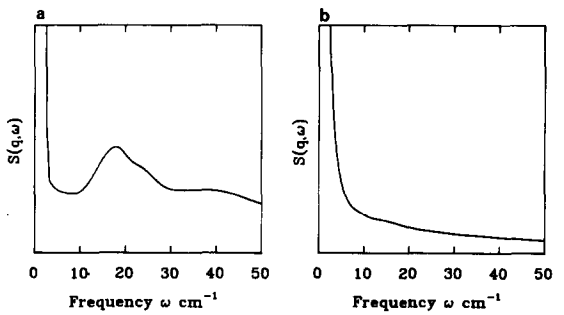

Fig. 7. $S(q, \omega)$ for myoglobin at 80 K (a) and 300 K (b) calculated from molecular dynamics simulations. The real part of the classical intermediate scattering function was evaluated by time averaging over the trajectory for each nonexchangeable hydrogen. That part of the correlation function involving times of up to half the trajectory length was used for calculation of $S(q, \omega)$ by numerical Fourier transformation. The contributions to $S(q, \omega)$ from all nonexchangeable hydrogens were summed. The detailed balance factor was included. The calculations were performed at constant $q = 1$ Å^{-1}, whereas the experimental data in fig. 6 is at constant angle. However, the basic form of the scattering, and the position of the vibrational peak is unaffected by this difference.

3. Conclusions

A combination of theoretical and neutron experimental work has allowed specific conclusions to be reached concerning the internal dynamics of proteins under different experimental conditions. A comparison of the spectra for lysozyme and BPTI (Figs. 1(a) and 1(b)) lends added support for the idea that the low frequency neutron spectra for different globular proteins under the same experimental conditions tend to be similar. This is true even for such structurally diverse molecules as the all β-sheet concanavalin-A [7] and the all-α helix myoglobin. This suggests that the frequency distribution associated with picosecond motions (though not necessarily the amplitude distribution) is largely independent of tertiary structure, and that results obtained with a single model protein may be generally applicable.

The basic form of the density of states at low hydrations or temperatures is explicable using harmonic dynamics. However, the calculated scattering is very sensitive to aspects of the harmonic model, as illustrated in fig. 2. The electrostatic truncation method and the extended atom approximation affect the calculated $g(\omega)$ such that we can clearly identify the normal modes calculated using 'switch' electrostatics and the all-atom representation as in best agreement with the experimental $G(\omega)$. As well as predicting a frequency distribution of the correct overall form, this model also predicts the amplitudes of the motions as a function of frequency in approximate agreement with experiment [12].

A possible reason for the smoothness of the curves in figs. 1(a) and 1(b), relative to the undamped theoretical time of flight spectrum shown in fig. 3, could be that the vibrational modes are damped by frictional effects within the protein. A model of the powder sample including overdamping of the lowest frequency modes (fig. 3) produces improved agreement with experiment. However, this is not the only possible explanation for the smoothness of the observed spectra. As discussed in section 2.5, it is likely that the protein exists in multiple conformational substates. For any individual substate the harmonic approximation may be a good representation of the low frequency dynamics [19]. However, the substates, which are associated with different potential energy minima, would have slightly different distributions of low frequency modes. This is expected to lead to noticeable smoothing of the observed spectra. The relative sharpness of the "harmonic" peak calculated from the 80 K myoglobin simulation, which is relatively localised in corformational space, might be due to this effect.

The measured spectra change markedly as a function of hydration and temperature. The experimental results indicate that, with increasing hydration, the average atomic amplitudes increase with a corresponding increase in the quasielastic scattering. This result is consistent with molecular dynamics studies [20, 21] and with a previous neutron experiment on lysozyme powders [22] which showed increased atomic amplitudes of motion and quasielastic effects with an increase of hydration from 0.06 g D_2O/g protein to 0.20 g D_2O/g protein. The relatively high hydration of the myoglobin powders (0.33 g D_2O/g protein) was sufficient to allow the 300 K scattering to be mostly quasielastic.

Our calculations suggest that a shift in the frequency distribution to low frequencies with increased frictional damping can reproduce the spectral change on hydration and increased temperature. However, transitions between substates may also be involved. An analysis of the myoglobin simulations [23] indicates that at 80 K the region of conformational space explored by the molecule is much smaller than at 300 K. Also, it has been shown by a simulation that, at 300 K, the rate of transitions between some of the conformational substates is on the picosecond timescale [18]. It is thus likely that at least part of the quasielastic scattering seen at 300 K is due to increased transitions between conformational substates, rather than damped harmonic modes.

We have demonstrated how combination of inelastic neutron scattering experiments and theoretical dynamical calculations can be used to gain insight into the low frequency dynamics of proteins. Clear effects of environmental conditions on the calculated spectra are manifest, but further theoretical and experimental work must be done to obtain a complete characterisation of the dynamical behaviour of globular proteins as a function of temperature and hydration.

Acknowledgements

We acknowledge Bayer AG for their kind gift of BPTI, Marc Bee and A.J. Dianoux for assistance with the experiments, and the Minnesota and John van Neumann supercomputer centres for the computations. The work was supported in part by a grant from the NSF(MK).

References

[1] C.L. Brooks, M. Pettitt and M. Karplus, Adv. Chem. Phys., in press.
[2] J.A. McCammon and S.C. Harvey, Dynamics of Macromolecules (Clarendon, Oxford, 1987).
[3] J. Smith, J.L. Finney and S. Cusack, in preparation.
[4] H.D. Middendorf, Ann. Rev. Biophys. Bioeng. 13 (1984) 425.
[5] S. Cusack, J. Smith, J. Finney, M. Karplus and J. Trewhella, Physica B 136 (1986) 256.
[6] H.D. Bartunik, P. Jollis, J. Berthou and A.J. Dianoux, Biopolymers 21 (1982) 43.
[7] S. Cusack, manuscript in preparation.
[8] J. Smith, S. Cusack, B. Brooks, U. Pezzeca and M. Karplus, J. Chem. Phys. 85 (1986) 3636.
[9] B.R. Brooks, R. Bruccoleri, B. Olafson, D. States, S. Swaminathan and M. Karplus, J. Comp. Chem. 4 (1983) 187.
[10] J. Deisenhofer and W. Steigemann, Acta Crystallogr. B 31 (1975) 238.
[11] B.R. Brooks and M. Karplus, Proc. Natl. Acad. Sci. U.S.A. 80 (1983) 6571.

[12] S. Cusack, J. Smith, J.L. Finney, B. Tidor and M. Karplus, J. Mol. Biol. 202 (1988) 903.
[13] J. Smith, S. Cusack, B. Tidor and M. Karplus, in preparation.
[14] S. Cusack, Comments Mol. Cell Biophys. 3 (1986) 243.
[15] S. Cusack and W. Doster, manuscript in preparation.
[16] A. Ansari, J. Berendzen, S.F. Bonze, H. Frauenfelder, I.E.T. Iben, T.B. Sauke, E. Shyamsunder and R. Young, Proc. Natl. Acad. Sci. U.S.A. 82 (1985) 5000.
[17] P.G. Debrunner and H. Frauenfelder, Ann. Rev. Phys. Chem. 33 (1982) 283.
[18] R. Elber and M. Karplus, Science 235 (1987) 318.
[19] T. Ichiye and M. Karplus, Proteins 2 (1987) 236.
[20] S. Swaminathan, T. Ichiye, W. van Gunsteren and M. Karplus, Biochemistry 21 (1982) 5230.
[21] W.F. van Gunsteren and M. Karplus, Biochemistry 21 (1982) 2259.
[22] J. Smith, S. Cusack, P. Poole and J. Finney, J. Biomol. Struct. Dyn. 4(4) (1987) 583.
[23] K. Kuczera, J. Kuriyan and M. Karplus, to be published.
[24] R. Scherm, C. Carlile, A.J. Dianoux, J. Suck and J. White, Institut Laue-Langevin Scientific Report 76S235S (1976).